10

Heat Transfer in Living Tissue

10.1 Introduction

The determination of temperature distribution in blood perfused tissue is important in many medical therapies and physiological studies. Examples are found in cryosurgery, frost bite, hyperthermia, skin burns and body thermal regulation and response to environmental conditions and during thermal stress. The key to thermal modeling of blood perfused tissue is the formulation of an appropriate heat transfer equation. Such an equation must take into consideration three factors: (1) blood perfusion, (2) the vascular architecture, and (3) variation in thermal properties and blood flow rate. The problem is characterized by anisotropic blood flow in a complex network of branching arteries and veins with changing size and orientation. In addition, blood is exchanged between artery-vein pairs through capillary bleed-off along vessel walls, draining blood from arteries and adding it to veins. Energy is transported between neighboring vessels as well as between vessels and tissue. Thus, heat transfer takes place in a blood perfused inhomogeneous matrix undergoing metabolic heat production. The search for heat equations modeling this complex process began over half a century ago and remains an active topic among current investigators. Over the years, several bioheat transfer equations have been formulated. A brief description of some of these equations will be presented and their limitations, shortcomings and applicability outlined. Before these equations are presented, related aspects of the vascular circulation network and blood flow and temperature patterns are summarized.

10.2 Vascular Architecture and Blood Flow

Blood from the heart is distributed to body tissues and organs through a system of vessels (arteries) that undergo many generations of branching

accompanied by diminishing size and flow rate. Because of their small size, vessels are measured in micrometers, $\mu = 10^{-6}$ m. This unit is also known as micron. Fig. 10.1 is a schematic diagram showing a typical vascular structure.

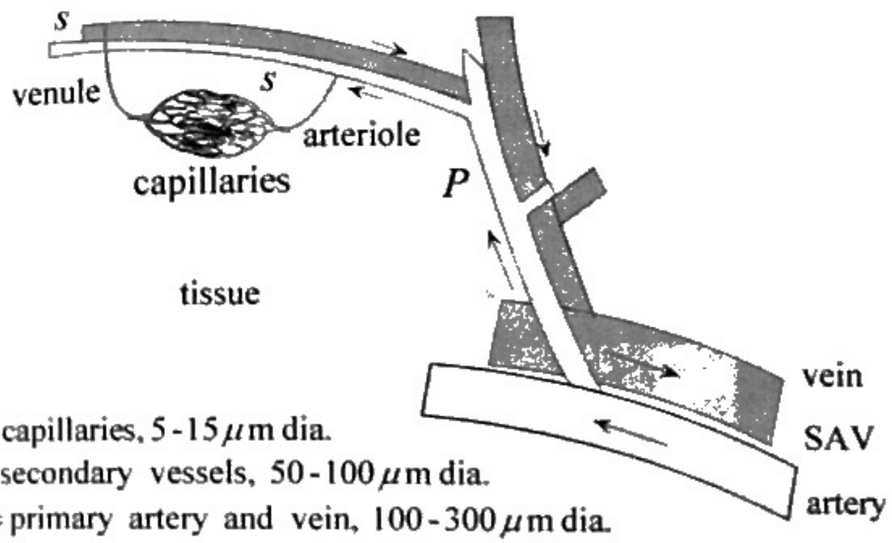

c = capillaries, 5 - 15 μm dia.
s = secondary vessels, 50 - 100 μm dia.
P = primary artery and vein, 100 - 300 μm dia.
SAV = main supply artery and vein, 300 - 1000 μm dia.

Fig. 10.1

Blood leaves the heart through the *aorta*, which is the largest artery (diameter $\approx$ 5,000 μm). Vessels supplying blood to muscles are known as *main supply arteries* and *veins* (*SAV*, 300 – 1000 μm diameter). They branch into *primary arteries*, (*P*, 100 – 300 μm diameter) which feed the *secondary arteries* (*s*, 50 – 100 μm diameter). These vessels deliver blood to the *arterioles* (20 – 40 μm diameter) which supply blood to the smallest vessels known as *capillaries* (5 – 15 μm diameter). Blood is returned to the heart through a system of vessels known as *veins*. For the most part they run parallel to the arteries forming pairs of counter current flow channels. The veins undergo confluence as they proceed from the capillaries to *venules*, *secondary veins* and to *primary veins*. Blood is returned to the heart through the *vena cava*, which is the largest vessel in the circulatory system. It should be noted that veins are larger than arteries by as much as 100%.

10.3 Blood Temperature Variation

Blood leaves the heart at the arterial temperature T_{a0}. It remains essentially at this temperature until it reaches the main arteries where equilibration with surrounding tissue begins to take place. Equilibration becomes complete prior to reaching the arterioles and capillaries where blood and tissue are at the same temperature T. Tissue temperature can be higher or lower than T_{a0}, depending on tissue location in the body. Blood returning from capillary beds near the skin is cooler than that from deep tissue layers. Blood mixing due to venous confluence from different tissue sources brings blood temperature back to T_{a0} as it returns to the heart via the vena cava. Fig. 10.2 is a schematic of blood temperature variation along the artery-vein paths.

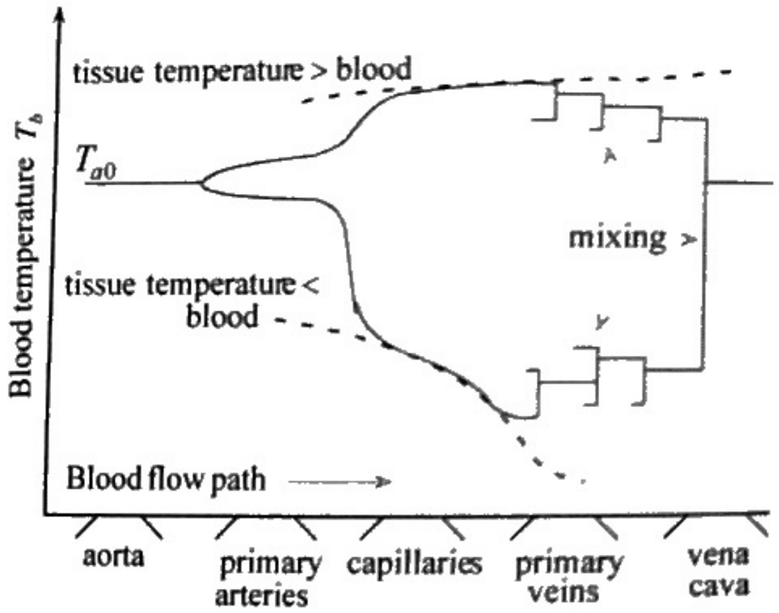

Fig. 10.2 Schematic of blood tempearature variation in vessels. (From [5] with permission.)

To maintain constant body temperature heat production due to metabolism must be continuously removed from the body. Blood circulation is a key mechanism for regulating body temperature. During conditions of thermal stress, blood flow to tissues under the skin increases. This results in higher rates of cooler venous blood which is used to bring the temperature of blood returning to the heart to its normal level.

10.4 Mathematical Modeling of Vessels-Tissue Heat Transfer

The complex nature of heat transfer in living tissue precludes exact mathematical modeling. Assumptions and simplifications must be made to make the problem tractable while capturing the essential features of the process. The following is an abridged review of various heat equations for the determination of temperature distribution in living tissues. We will begin with the Pennes bioheat equation which was published in 1948. What is attractive and remarkable about this equation is its simplicity and applicability under certain conditions. Nevertheless, to address its shortcomings, several investigators have formulated alternate equations to model heat transfer in living tissues. In each case the aim was to refine the Pennes equation by accounting for factors that are known to play a role in the process. Improvements have come at the expense of mathematical complexity and/or dependency on vascular geometry data, blood perfusion and thermal properties. Detailed derivation and discussion of all equations is beyond the scope of this chapter. Instead five selected models will be presented and their main features identified.

10.4.1 Pennes Bioheat Equation [1]

(a) Formulation

Pennes bioheat equation is based on simplifying assumptions concerning the following four central factors:

(1) *Equilibration Site*. The principal heat exchange between blood and tissue takes place in the capillary beds, the arterioles supplying blood to the capillaries and the venules draining it. Thus all pre-arteriole and post-venule heat transfer between blood and tissue is neglected.

(2) *Blood Perfusion*. The flow of blood in the small capillaries is assumed to be isotropic. This neglects the effect of blood flow directionality.

(3) *Vascular Architecture*. Larger blood vessels in the vicinity of capillary beds play no role in the energy exchange between tissue and capillary blood. Thus the Pennes model does not consider the local vascular geometry.

(4) *Blood Temperature*. Blood is assumed to reach the arterioles supplying the capillary beds at the body core temperature T_{a0}. It instantaneously exchanges energy and equilibrates with the local tissue temperature T. Based on these assumptions, Pennes [1]

modeled blood effect as an isotropic heat source or sink which is proportional to blood flow rate and the difference between body core temperature T_{a0} and local tissue temperature T. In this model, blood originating at temperature T_{a0} does not experience energy loss or gain as it flows through long branching arteries leading to the arterioles and capillaries. Using this idealized process the contribution of blood to the energy balance can be quantified.

Consider the blood perfused tissue element shown in Fig. 10.3. The element is large enough to be saturated with arterioles, venules and capillaries but small compared to the characteristic dimension of the region under consideration. This tissue-vessels matrix is treated as a continuum whose collective temperature is T. Following the formulation of the heat conduction equation of Section 1.4, energy conservation for the element is given by eq. (1.6)

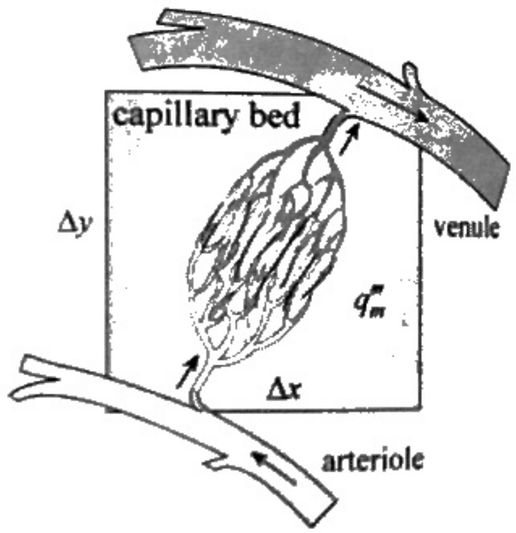

Fig. 10.3

$$\dot{E}_{in} + \dot{E}_g - \dot{E}_{out} = \dot{E}\,. \tag{1.6}$$

In Section 1.4 the rate of energy added to the element is by conduction and convection (mass motion). Here the convection component is eliminated and replaced by energy added due to blood perfusion. The simplest way to account for this effect is to treat it as energy generation $\dot{E}_g$. Let

q_b''' = net rate of energy added by the blood per unit volume of tissue
q_m''' = rate of metabolic energy production per unit volume of tissue

Thus equation (b) of Section 1.4 becomes

$$\dot{E}_g = q'''dxdydz = (q_b''' + q_m''')dxdydz\,. \tag{a}$$

To formulate an expression for q_b''' consider the elements shown in Fig. 10.3. According to Pennes, blood enters the element at the body

core temperature T_{a0}, it instantaneously equilibrates and exists at the temperature of the element T. Thus

$$q_b''' = \rho_b c_b \dot{w}_b (T_{a0} - T)\,, \tag{10.1}$$

where

c_b = specific heat of blood
$\dot{w}_b$ = blood volumetric flow rate per unit tissue volume
ρ_b = density of blood

Substituting eq. (10.1) into (a)

$$q''' = q_m''' + \rho_b c_b \dot{w}_b (T_{a0} - T)\,. \tag{10.2}$$

Returning to the heat conduction equation (1.7), we eliminate the convection terms (set $U = V = W = 0$) and use eq. (10.2) to obtain

$$\nabla \cdot k\nabla T + \rho_b c_b \dot{w}_b (T_{a0} - T) + q_m''' = \rho c \frac{\partial T}{\partial t}, \tag{10.3}$$

where

c = specific heat of tissue
k = thermal conductivity of tissue
ρ = density of tissue

The first term in eq. (10.3) represents conduction in the three directions. It takes the following forms depending on the coordinate system:

Cartesian coordinates:

$$\nabla \cdot k\nabla T = \frac{\partial}{\partial x}\left(k\frac{\partial T}{\partial x}\right) + \frac{\partial}{\partial y}\left(k\frac{\partial T}{\partial y}\right) + \frac{\partial}{\partial z}\left(k\frac{\partial T}{\partial z}\right). \tag{10.3a}$$

Cylindrical coordinates:

$$\nabla \cdot k\nabla T = \frac{1}{r}\frac{\partial}{\partial r}\left(kr\frac{\partial T}{\partial r}\right) + \frac{1}{r^2}\frac{\partial}{\partial \theta}\left(k\frac{\partial T}{\partial \theta}\right) + \frac{\partial}{\partial z}\left(k\frac{\partial T}{\partial z}\right). \tag{10.3b}$$

Spherical coordinates:

$$\nabla \cdot k\nabla T = \frac{1}{r^2}\frac{\partial}{\partial r}\left(kr^2\frac{\partial T}{\partial r}\right) + \frac{1}{r^2 \sin\phi}\frac{\partial}{\partial \phi}\left(k\sin\frac{\partial T}{\partial \phi}\right) + \frac{1}{r^2\sin^2\phi}\frac{\partial}{\partial \theta}\left(k\frac{\partial T}{\partial \theta}\right). \tag{10.3c}$$

Equation (10.3) is known as the *Pennes bioheat equation*. Note that the mathematical role of the perfusion term in Pennes's equation is identical to the effect of surface convection in fins, as shown in equations (2.5), (2.19), (2.23) and (2.24). The same effect is observed in porous fins with coolant flow (see problems 5.12, 5.17, and 5.18).

(b) Shortcomings

The Pennes equation has been the subject of extensive study and evaluation [2-11]. The following gives a summary of critical observations made by various investigators. Attention is focused on the four assumptions made in the formulation of the Pennes equation. Discrepancy between theoretical predictions and experimental results is traced to these assumptions.

(1) *Equilibration Site*. Thermal equilibration does not occur in the capillaries, as Pennes assumed. Instead it takes place in pre-arteriole and post-venule vessels having diameters ranging from $70-500\,\mu m$ [3-5]. This conclusion is based on theoretical determination of the *thermal equilibration length*, L_e, which is the distance blood travels along a vessel for its temperature to equilibrate with the local tissue temperature. For arterioles and capillaries this distance is much shorter than their length L. Vessels for which $L_e / L > 1$ are commonly referred to as *thermally significant*.

(2) *Blood Perfusion*. Directionality of blood perfusion is an important factor in the interchange of energy between vessels and tissue. The Pennes equation does not account for this effect. Capillary blood perfusion is not isotropic but proceeds from arterioles to venules.

(3) *Vascular Architecture*. Pennes equation does not consider the local vascular geometry. Thus significant features of the circulatory system are not accounted for. This includes energy exchange with large vessels, countercurrent heat transfer between artery-vein pairs and vessel branching and diminution.

(4) *Blood Temperature*. The arterial temperature varies continuously from the deep body temperature of the aorta to the secondary arteries supplying the arterioles, and similarly for the venous return. Thus, contrary to Pennes' assumption, pre-arteriole blood temperature is not equal to body core temperature T_{a0} and vein return temperature is not

equal to the local tissue temperature T. Both approximations overestimate the effect of blood perfusion on local tissue temperature.

(c) Applicability

Despite the serious shortcomings of the Pennes equation it has enjoyed surprising success in many applications such as hyperthermia therapy, blood perfusion measurements, cryosurgery and thermal simulation of whole body. In some cases analytical results are in reasonable agreement with experimental data. Studies have shown that the Pennes equation is applicable in tissue regions where vessel diameters are greater than $500\,\mu m$ and for which equilibration length to total length L_e / L is greater than 0.3 [6].

Example 10.1: Temperature Distribution in the Forearm

Model the forearm as a cylinder of radius R with volumetric blood perfusion rate per unit tissue volume $\dot{w}_b$ and metabolic heat production q'''_m. The arm surface exchanges heat with the surroundings by convection. The heat transfer coefficient is h and the ambient temperature is T_∞. Use Pennes bioheat equation to determine the steady state one-dimensional temperature distribution in the arm.

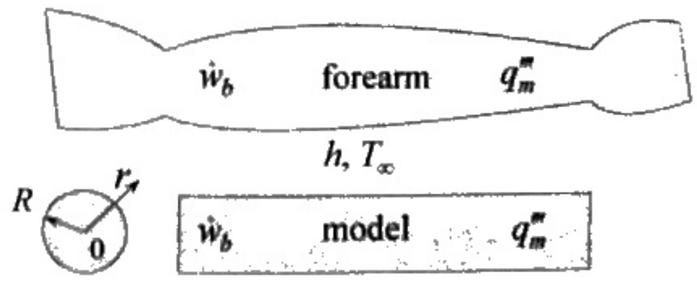

Fig. 10.4

(1) Observations. (i) The forearm can be modeled as a cylinder with uniform energy generation. (ii) Heat is transported to the surface by conduction and removed from the surface by convection. (iii) In general, temperature variation in the forearm is three-dimensional.

(2) Origin and Coordinates. Fig. 10.4 shows the origin and the radial coordinate r.

(3) Formulation.

(i) Assumptions. (1) Steady state, (2) the forearm can be modeled as a constant radius cylinder, (3) bone and tissue have the same properties and are uniform throughout, (4) uniform metabolic heat production, (5) uniform blood perfusion, (5) no variation in the angular direction, (6) negligible axial conduction, (7) skin layer is neglected and (8) Pennes bioheat equation is applicable.

(ii) Governing Equations. Pennes bioheat equation (10.3) for one-dimensional steady state radial heat transfer simplifies to

$$\frac{1}{r}\frac{d}{dr}\left(r\frac{dT}{dr}\right)+\frac{\rho_b c_b \dot{w}_b}{k}(T_{a0}-T)+\frac{q_m'''}{k}=0. \tag{a}$$

(iii) Boundary Conditions. Temperature symmetry and convection at the surface give the following two boundary conditions:

$$\frac{dT(0)}{dr}=0, \text{ or } T(0)=\text{finite}, \tag{b}$$

$$-k\frac{dT(R)}{dr}=h[T(R)-T_\infty]. \tag{c}$$

(4) Solution. Eq.(a) is rewritten in dimensionless form using the following dimensionless variables

$$\theta=\frac{T-T_{a0}}{T_\infty-T_{a0}}, \quad \xi=\frac{r}{R}. \tag{d}$$

Substituting (d) into (a)

$$\frac{1}{\xi}\frac{d}{d\xi}\left(\xi\frac{d\theta}{d\xi}\right)-\frac{\rho_b c_b \dot{w}_b R^2}{k}\theta-\frac{q_m''' R^2}{k(T_{a0}-T_\infty)}=0. \tag{e}$$

The coefficient of the second term in (e) is a dimensionless parameter representing the effect of blood flow. Let

$$\beta=\frac{\rho_b c_b \dot{w}_b R^2}{k}. \tag{f}$$

The last term in (e) is a parameter representing the effect of metabolic heat. Let

$$\gamma=\frac{q_m''' R^2}{k(T_{a0}-T_\infty)}. \tag{g}$$

Substituting (f) and (g) into (e)

$$\frac{1}{\xi}\frac{d}{d\xi}\left(\xi\frac{d\theta}{d\xi}\right)-\beta\theta-\gamma=0. \tag{h}$$

Boundary conditions (b) and (c) are similarly expressed in dimensionless form

$$\frac{d\theta(0)}{d\xi}=0, \text{ or } \theta(0)=\text{finite}, \tag{i}$$

$$-\frac{d\theta(1)}{d\xi}=Bi[\theta(1)-1], \tag{j}$$

where Bi is the Biot number defined as

$$Bi=\frac{hR}{k}.$$

The homogeneous part of equation (h) is a Bessel differential equation. The solution to (h) is

$$\theta(\xi)=C_1 I_0(\sqrt{\beta}\xi)+C_2 K_0(\sqrt{\beta}\xi)-\frac{\gamma}{\beta}, \tag{k}$$

where C_1 and C_2 are constants of integration. Boundary conditions (i) and (j) give

$$C_1=\frac{Bi[1+(\gamma/\beta)]}{\sqrt{\beta}\,I_1(\sqrt{\beta})+Bi\,I_0(\sqrt{\beta})}, \quad C_2=0. \tag{m}$$

Substituting (m) into (k) gives

$$\theta(r)=\frac{T(r)-T_{a0}}{T_\infty-T_{a0}}=\frac{Bi[1+(\gamma/\beta)]}{\sqrt{\beta}\,I_1(\sqrt{\beta})+Bi\,I_0(\sqrt{\beta})}I_0(\sqrt{\beta}\,r/R)-\frac{\gamma}{\beta}. \tag{n}$$

(5) Checking. *Dimensional check*: The parameters Bi, β and γ are dimensionless. Thus the arguments of the Bessel functions and each term in solution (n) are dimensionless.

Limiting check: If no heat is removed by convection ($h = 0$), the entire arm reaches a uniform temperature T_o and all energy generation due to metabolic heat is transferred to the blood. Conservation of energy for the blood gives

$$q_m''' = \rho_b c_b \dot{w}_b (T_o - T_{a0}) .$$

Solving for T_o

$$T_o = T_{a0} + \frac{q_m'''}{\rho_b c_b \dot{w}_b} . \qquad \text{(o)}$$

Setting $h = Bi = 0$ in (n)

$$T(r) = T_{a0} + \frac{q_m'''}{\rho_b c_b \dot{w}_b} . \qquad \text{(p)}$$

This agrees with (o).

(6) Comments. (1) The solution is characterized by three parameters: surface convection *Bi*, metabolic heat γ, and blood perfusion parameter β. (2) Setting $r = 0$ and $r = R$ in (n) gives the center and surface temperatures, respectively. (3) The solution corresponding to zero metabolic heat production is obtained by setting $q_m''' = \gamma = 0$. However, the solution for zero blood perfusion rate can not be deduced from (n) since setting $\beta = 0$ in (n) gives terms of infinite magnitude. This is due to the fact that β appears in differential equation (h) as a coefficient of the variable θ. To obtain a solution for zero perfusion one must first set $\beta = 0$ in (h) and then solve the resulting equation. This procedure gives

$$\frac{T - T_\infty}{(R^2 q_m''' / k)} = \frac{1}{2Bi} + \frac{1}{4}\left[1 - (r/R)^2\right]. \qquad \text{(q)}$$

The two solutions, (n) and (q), make it possible to examine the effect of blood perfusion relative to metabolic heat production on the temperature distribution.

10.4.2 Chen-Holmes Equation [5]

An important development in the evolution of bioheat transfer modeling is the demonstration by Chen and Holmes that blood equilibration with the tissue occurs prior to reaching the arterioles. Based on this finding they modified Pennes perfusion term, taking into consideration blood flow

directionality and vascular geometry, and formulated the following equation

$$\nabla \cdot k\nabla T + \dot{w}_b^* \rho_b c_b (T_a^* - T) - \rho_b c_b \bar{u} \cdot \nabla T + \nabla \cdot k_p \nabla T + q_m = \rho c \frac{\partial T}{\partial t} . \qquad (10.4)$$

Although the second term in this equation appears similar to Pennes' perfusion term, it is different in two respects: (1) $\dot{w}_b^*$ is the perfusion rate at the *local* generation of vessel branching and (2) T_a^* is not equal to the body core temperature. It is essentially the temperature of blood upstream of the arterioles. The third term in eq. (10.4) accounts for energy convected due to equilibrated blood. Directionality of blood flow is described by the vector $\bar{u}$, which is the volumetric flow rate per unit area. This term is similar to the convection term encountered in moving fins and in flow through porous media (see equations (2.19) and (5.6)). The fourth term in eq. (10.4) describes conduction mechanisms associated with small temperature fluctuations in equilibrated blood. The symbol k_p denotes "perfusion conductivity". It is a function of blood flow velocity, vessel inclination angle relative to local temperature gradient, vessel radius and number density.

In formulating eq. (10.4) mass transfer between vessels and tissue is neglected and thermal properties k, c and ρ are assumed to be the same as those of the solid tissue. Other assumptions limit the applicability of this equation to vessels that are smaller than 300 μm in diameter and equilibration length ratio $L_e / L < 0.6$.

Although the Chen-Holmes model represents a significant improvement over Pennes' equation, its application requires detailed knowledge of the vascular network and blood perfusion. This makes it difficult to use. Nevertheless, the model met with some success in predicting temperature distribution in the pig kidney.

10.4.3 Three-Temperature Model for Peripheral Tissue [7]

Since blood perfused tissue consists of three elements: arteries, veins and tissue, it follows that to rigorously analyze heat transfer in such a medium it is necessary to assign three temperature variables: arterial temperature T_a, venous T_v and tissue T. This approach was followed in analyzing the

peripheral tissue of a limb schematically shown in Fig. 10.5 [7]. Three vascular layers were identified: deep layer, intermediate and cutaneous layers. The deep layer is characterized by countercurrent artery-vein pairs that are thermally significant. The intermediate layer is modeled as a porous media exchanging heat with pairs of thermally significant vessels. The thin cutaneous layer just below the skin is independently supplied by countercurrent artery-vein vessels called *cutaneous plexus*. Blood supply to the cutaneous layer is controlled through vasodilation and vasoconstriction of the cutaneous plexus. This is an important mechanism for regulating surface heat flux. This layer is divided into two regions; an upper region with negligible blood effect and a lower region having uniform blood perfusion heat source similar to the Pennes term.

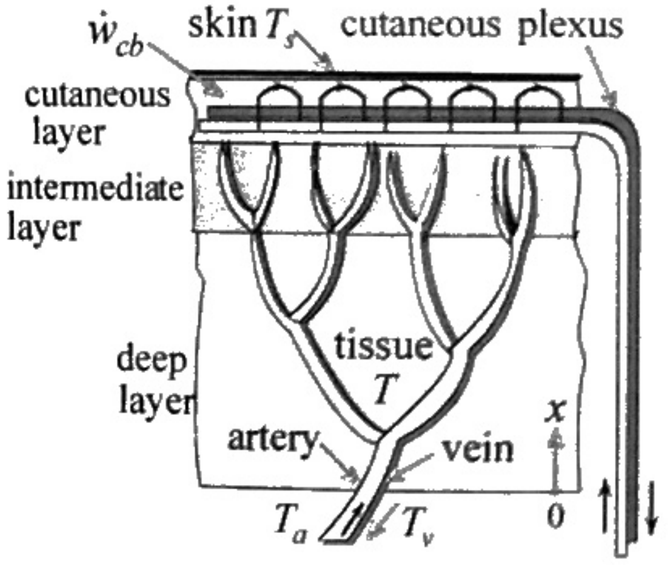

Fig. 10.5

A total of seven governing equations were formulated: three coupled equations for the deep layer, two for the intermediate and two for the cutaneous. Although this model accounts for the vascular geometry and blood flow directionality, solutions to the set of seven equations require numerical integration as well as detailed vascular data. Nevertheless, it was applied to peripheral tissue to examine the effect of various parameters [12]. It was also used to evaluate the performance of other models [6].

Formulation of the three-temperature equations for the deep layer will not be presented here since a simplified form will be outlined in the following section. However, attention is focused on the cutaneous layer. The one-dimensional steady state heat equation for the lower region is given by

$$\frac{d^2T_1}{dx^2} + \frac{\rho_b c_b \dot{w}_{cb}}{k}(T_{c0} - T_1) = 0, \tag{10.5}$$

where

T_1 = temperature distribution in the lower region of the cutaneous layer
T_{c0} = temperature of blood supplying the cutaneous pelxus
$\dot{w}_{cb}$ = cutaneous layer volumetric blood perfusion rate per unit tissue volume
x = coordinate normal to skin surface

The upper region of the cutaneous layer just under the skin surface is governed by pure conduction. Thus the one-dimensional steady state heat equation for this region is

$$\frac{d^2T_2}{dx^2} = 0, \tag{10.6}$$

where

T_2 = temperature distribution in the upper region of the cutaneous layer

10.4.4 Weinbaum-Jiji Simplified Bioheat Equation for Peripheral Tissue [8]

Recognizing the complexity of the three-temperature model, Weinbaum and Jiji [8] introduced simplifications reducing the three coupled deep layer equations for T_a, T_v and T to a single equation for the tissue temperature. Although the simplified form retains the effect of vascular geometry and accounts for energy exchange between artery, vein and tissue, the added approximations narrow its applicability. A brief description of this bioheat equation follows.

Fig. 10.6 shows a control volume containing a finite number of artery-vein pairs. Blood flow in each pair is in opposite direction (countercurrent). In addition, artery blood temperature T_a is different from vein temperature T_v. Thus, these vessels are *thermally significant* (not in thermal equilibrium). Not shown in Fig.10.6 are

numerous *thermally insignificant* capillaries, arterioles, and venules that saturate the tissue. In formulating conservation of energy for the tissue within the control volume, one must take into consideration the following: (1) Conduction through the tissue. (2) Energy exchange by conduction between vessel pairs and tissue. Note that heat conduction from the artery to the tissue is not equal to conduction from the tissue to the vein. This imbalance is described as *incomplete countercurrent exchange*. (3) Energy exchange between vessels and tissue due to capillary blood bleed-off from artery to vein.

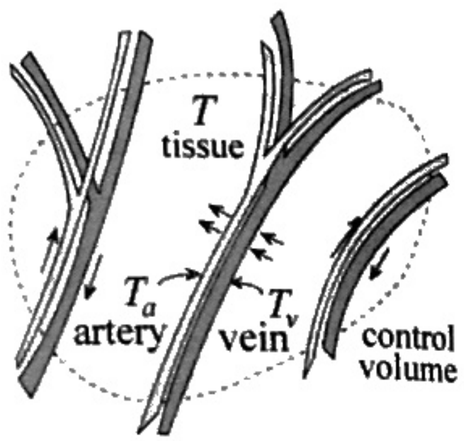

Fig. 10.6

(a) Assumptions. Key assumptions in the simplified bioheat equation are: (1) blood bleed-off rate leaving the artery is equal to that returning to vein and is uniformly distributed along each pair, (2) bleed-off blood leaves the artery at T_a and enters the vein at the venous blood temperature T_v, (3) artery and vein have the same radius, (4) negligible axial conduction through vessels, (5) equilibration length ratio $L_e / L << 1$ and (6) tissue temperature T is approximated by the average of the local artery and vein temperatures. That is

$$T \approx (T_a + T_v)/2 . \tag{10.7}$$

(b) Formulation. Based on the above assumptions, application of conservation of mass for the artery and vein and conservation of energy for the artery, vein and tissue in the control volume, give the simplified bioheat equation for tissue temperature. For the special one-dimensional case where blood vessels and temperature gradient are in the same direction x, the equation reduces to [8]

$$\rho c \frac{\partial T}{\partial t} = \frac{\partial}{\partial x}\left(k_{eff} \frac{\partial T}{\partial x}\right) + q'''_m , \tag{10.8}$$

where k_{eff} is the *effective conductivity*, defined as

$$k_{eff} = k\left[1 + \frac{n}{k^2\sigma}(\pi \rho_b c_b a^2 u)^2\right], \tag{10.9}$$

were

a = vessel radius
n = number of vessel pairs crossing control volume surface per unit area
u = average blood velocity in countercurrent artery or vein
σ = shape factor, defined in eq. (10.10)

The shape factor σ is associated with the resistance to heat transfer between two parallel vessels embedded in an infinite medium. For the case of vessels at uniform surface temperatures with center to center spacing l, the shape factor is given by [13]

$$\sigma = \frac{\pi}{\cosh(l/2a)}. \tag{10.10}$$

Equation (10.9) shows that k_{eff} reflects the effects of vascular geometry and blood perfusion on tissue temperature. It is useful to separate these two effects so that their roles can be analyzed individually. The variables a, σ, n and u depend on the vascular geometry. Using conservation of mass, the local blood velocity u can be expressed in terms of the inlet velocity u_o to the tissue layer and the vascular geometry. Thus, eq. (10.9) is rewritten as

$$k_{eff} = k\left[1 + \frac{(2\rho_b c_b a_o u_o)^2}{k_b^2} V(\xi)\right], \tag{10.11}$$

where

a_o = vessel radius at the inlet to the tissue layer at $x = 0$
$V(\xi)$ = dimensionless vascular geometry function
$\xi = x/L$ = dimensionless distance
L = tissue layer thickness
u_o = blood velocity at the inlet to the tissue layer at $x = 0$

Given the vascular data the function $V(\xi)$ can be constructed. It is important to note that this function is independent of blood perfusion. In addition, the coefficient $(2\rho_b c_b a_o u_o / k_b)$ which characterizes blood flow rate is independent of the vascular geometry. It represents the inlet Peclet number, which is the product of Reynolds and Prandtl numbers, defined as

$$Pe_o = \frac{2\rho_b c_b a_o u_o}{k_b}. \tag{10.12}$$

Substituting eq. (10.12) into eq. (10.11) gives

$$k_{eff} = k\left[1 + Pe_o^2 V(\xi)\right]. \tag{10.13}$$

The following observations are made regarding the definition of effective conductivity k_{eff}

(1) For the more general three-dimensional case, the orientation of vessel pairs relative to the direction of the local tissue temperature gradient gives rise to a tensor conductivity that has similar properties to an anisotropic material [8].

(2) The second term on the right hand side of eqs. (10.11) and (10.13) represents the enhancement in tissue conductivity. This enhancement is due to countercurrent convection in the thermally significant microvessel pairs and capillary blood bleed-off.

The two regions of the cutaneous layer shown in Fig. 10.5 are governed by equations (10.5) and (10.6). However, for consistency with the formulation of k_{eff} in the tissue layer, eq. (10.5) will be expressed in terms of the Peclet number Pe_0. Blood perfusion rate $\dot{w}_b$ in the tissue layer is given by

$$\dot{w}_b = \frac{\pi n_o a_o^2 u_o}{L}, \tag{10.14}$$

where n_o is the number of arteries entering the tissue layer per unit area. Substituting eq. (10.12) into eq. (10.14) gives

$$\dot{w}_b = \frac{\pi n_o a_o k_b}{2L\rho_b c_b} Pe_o. \tag{10.15}$$

Define R as the ratio of *total* rate of blood supplied to the cutaneous layer to the *total* rate of blood supplied to the tissue layer. Thus

$$R = \frac{L_1 \dot{w}_{cb}}{L\,\dot{w}_b}, \tag{10.16}$$

where L_1 is the thickness of the cutaneous layer. Substituting eqs. (10.15) and (10.16) into eq. (10.5) gives

$$\frac{d^2T_1}{dx^2} + \frac{\pi n_o a_o k_b}{2kL_1} RPe_0(T_{c0} - T_1) = 0. \tag{10.17}$$

(c) Limitation and Applicability. To test the validity of assumptions made in formulating eq. (10.8), numerical results using the solution to this equation were compared with those obtained from the solution to the three-temperature model developed in [7] and summarized in Section 10.4.3. The comparison was made for a simplified representation of one-dimensional heat transfer in the limb [6]. Results indicate that eq. (10.8) gives accurate predictions of tissue temperature for vessels smaller than 200 μm in diameter and equilibration length ratio $L_e/L < 0.3$. Experimental measurements on the rat spinotrapezius muscle showed that eq. (10.8) is valid for $L_e/L < 0.2$ [14]. It should be noted that the upper limit on vessel size decreases sharply under conditions of exercise due to an increase in blood flow rate.

Formulation of eq. (10.8) is based on vascular architecture characteristics of peripheral tissues less than 2 cm thick. It does not apply to deeper layers and to skeletal muscles where the vascular geometry takes on a different configuration.

Example 10.2: Temperature Distribution in Peripheral Tissue.

Consider the peripheral tissue shown schematically in Fig.10.5. Tissue thickness is L and skin surface is maintained at uniform temperature T_s. Blood at T_{a0} is supplied to the thermally significant arteries at $x = 0$. During resting state and neutral environment the effect of blood flow through the cutaneous layer is negligible. Consequently heat transfer through this layer is essentially by conduction. A representative vascular geometry function $V(\xi)$, shown in Fig. 10.7, for a typical peripheral tissue can be approximated by [15]

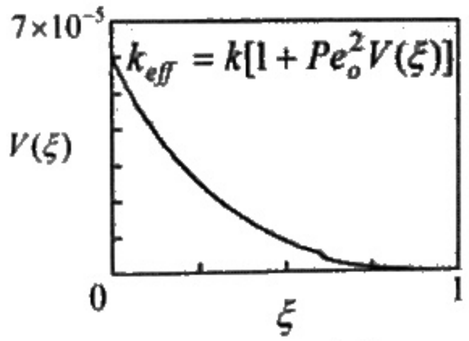

Fig. 10.7

$$V(\xi) = A + B\xi + C\xi^2,$$

where A, B and C are constants:

$$A = 6.32\times10^{-5},\ B = -15.9\times10^{-5}\ and\ C = 10\times10^{-5}.$$

Use the Weinbaum-Jiji simplified bioheat equation to obtain a solution to the temperature distribution in the tissue. Express the results in dimensionless form in terms of the following dimensionless quantities:

$$\xi = x/L,\quad \theta = \frac{T-T_s}{T_{a0}-T_s},\quad Pe_0 = \frac{2\rho_b c_b a_o u_o}{k_b},\quad \gamma = \frac{q_m''' L^2}{k(T_{a0}-T_s)}.$$

Construct a plot showing the effect of blood flow rate (Peclet number Pe_0) and metabolic heat production γ on tissue temperature $\theta(\xi)$. Note that an increase in γ brings about an increase in Pe_0. Compare $\theta(\xi)$ for $Pe_0 = 60$ and $\gamma = 0.02$ (resting state) with $Pe_0 = 180$ and $\gamma = 0.6$ (moderate exercise).

(1) Observations. (i) The variation of conductivity with distance along the three layers shown in Fig. 10.5 is known. (ii) The tissue can be modeled as a single layer with variable effective conductivity and constant energy generation due to metabolic heat. (iii) Tissue temperature increases as blood perfusion and/or metabolic heat are increased.

(2) Origin and Coordinates. Fig. 10.8 shows the origin and coordinate x.

(3) Formulation.

(i) Assumptions. (1) All assumptions leading to eqs. (10.8) and (10.9) are applicable, (2) steady state, (3) one-dimensional, (4) tissue temperature at the base $x = 0$ is equal to T_{a0}, (5) skin is maintained at uniform temperature and (6) negligible blood perfusion in the cutaneous layer.

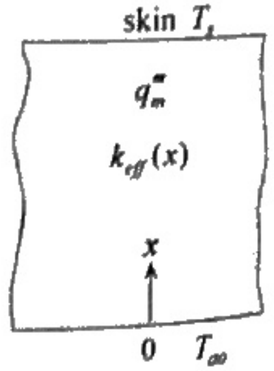

Fig. 10.8

(ii) Governing Equations. The bioheat equation for this model is obtained from eq. (10.8)

$$\frac{d}{dx}\left(k_{eff}\frac{dT}{dx}\right) + q_m''' = 0, \qquad \text{(a)}$$

where k_{eff} is defined in eq. (10.13) as

$$k_{eff} = k\left[1 + Pe_0^2\, V(\xi)\right], \qquad \text{(b)}$$

where k is tissue conductivity corresponding to zero blood perfusion enhancement and $V(\xi)$ is specified as

$$V(\xi) = A + B\xi + C\xi^2. \qquad \text{(c)}$$

(iii) Boundary Conditions. The two required boundary conditions are

$$T(0) = T_{a0}, \qquad \text{(d)}$$

$$T(L) = T_s. \qquad \text{(e)}$$

(4) Solution. To express the problem in non-dimensional form the following dimensionless quantities are defined:

$$\xi = \frac{x}{L},\quad \theta = \frac{T-T_s}{T_{a0}-T_s},\quad \gamma = \frac{q_m''' L^2}{k(T_{a0}-T_s)}. \qquad \text{(f)}$$

Substituting (b), (c) and (f) into (a) gives

$$\frac{d}{d\xi}\left[\left\{1 + Pe_0^2(A + B\xi + C\xi^2)\right\}\frac{d\theta}{d\xi}\right] + \gamma = 0. \qquad \text{(g)}$$

Boundary conditions (d) and (e) transform to

$$\theta(0) = 1, \qquad \text{(h)}$$

$$\theta(1) = 0. \qquad \text{(i)}$$

Integrating (g) once

$$\left[1 + Pe_0^2(A + B\xi + C\xi^2)\right]\frac{d\theta}{d\xi} = C_1 - \gamma\xi.$$

Separating variables and integrating again

$$\theta = C_1\int\frac{d\xi}{1 + Pe_0^2(A + B\xi + C\xi^2)} - \gamma\int\frac{\xi\, d\xi}{1 + Pe_0^2(A + B\xi + C\xi^2)} + C_2, \qquad \text{(j)}$$

where C_1 and C_2 are constants of integration. The two integrals in (j) are of the form

$$\int\frac{d\xi}{a + b\xi + c\xi^2} \text{ and } \int\frac{\xi\, d\xi}{a + b\xi + c\xi^2}, \qquad \text{(k)}$$

where the coefficients a, b and c are defined as

$$a = 1 + APe_0^2,\quad b = BPe_0^2,\quad c = CPe_0^2. \qquad \text{(m)}$$

Evaluating the two integrals analytically and substituting into (j) give the solution to θ

$$\theta = \frac{2C_1}{\sqrt{d}}\tan^{-1}\frac{b+2c\xi}{\sqrt{d}} - \frac{\gamma}{c}\left[\frac{1}{2}\ln(a+b\xi+c\xi^2) - \frac{b}{\sqrt{d}}\tan^{-1}\frac{b+2c\xi}{\sqrt{d}}\right] + C_2, \tag{n}$$

where

$$d = 4ac - b^2. \tag{o}$$

Boundary conditions (h) and (i) give the constants C_1 and C_2. The solution to θ becomes

$$\theta = 2\frac{C_1}{\sqrt{d}}\left[\tan^{-1}\frac{b+2c\xi}{\sqrt{d}} - \tan^{-1}\frac{b+2c}{\sqrt{d}}\right] - \frac{\gamma}{c}\left\{\frac{1}{2}\ln\frac{a+b\xi+c\xi^2}{a+b+c} - \frac{b}{\sqrt{d}}\left[\tan^{-1}\frac{b+2c\xi}{\sqrt{d}} - \tan^{-1}\frac{b+2c}{\sqrt{d}}\right]\right\}, \tag{p}$$

where the constant C_1 is given by

$$C_1 = \frac{1 - \frac{\gamma}{c}\left\{\frac{1}{2}\ln\frac{a+b+c}{a} + \frac{b}{\sqrt{d}}\left[\tan^{-1}\frac{b}{\sqrt{d}} - \tan^{-1}\frac{b+2c}{\sqrt{d}}\right]\right\}}{\frac{2}{\sqrt{d}}\left[\tan^{-1}\frac{b}{\sqrt{d}} - \tan^{-1}\frac{b+2c}{\sqrt{d}}\right]}. \tag{q}$$

Table 10.1

	Pe_o	
	60	180
a	1.2275	3.0477
b	-0.5724	-5.1516
c	0.36	3.24
d	1.44	12.96

Table 10.2

	k_{eff}/k	
ξ	$Pe_o = 60$	$Pe_o = 180$
0	1.44	3.05
0.2	1.13	2.15
0.4	1.06	1.51
0.6	1.01	1.12
0.8	1.00	1.02
1.0	1.02	1.14

The constants a, b, c and d depend on Pe_0. They are listed in Table 10.1. The constant C_1 depends on both Pe_o and γ. For $Pe_0 = 60$ and $\gamma = 0.02$ eq.(q) gives $C_1 = -1.047$ and for $Pe_0 = 180$ and $\gamma = 0.6$ it gives $C_1 = -1.0176$. Table 10.2 lists the enhancement in conductivity for the two values of Pe_0. Fig. 10.9 shows the corresponding temperature distribution.

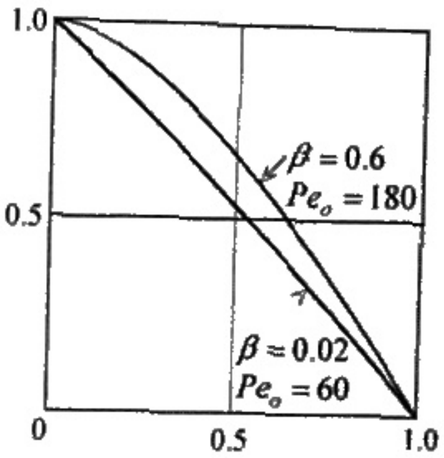

Fig. 10.9

(5) Checking. *Dimensional check*: Solution θ, metabolic heat parameter γ, Peclet number Pe_0 and the arguments of $\tan^{-1}$ and log are dimensionless.

Boundary conditions check: Solution (p) satisfies boundary conditions (*h*) and (i).

Qualitative check: As anticipated, Fig. 10.9 shows that tissue temperature increases as blood perfusion and metabolic heat are increased.

(6) Comments. (i) Table 10.2 shows the enhancement in k_{eff} due to blood perfusion. Increasing perfusion rate (Pe_0) increases k_{eff}. However, the enhancement diminishes rapidly towards the end of the tissue layer ($\xi = 0.8$). (ii) Fig. 10.9 shows that temperature distribution for $Pe_0 = 60$ and $\gamma = 0.02$ is nearly linear. The slight departure from linearity is due to metabolic heat production. For $Pe_0 = 180$ and $\gamma = 0.6$ tissue temperature is higher. The increase in temperature is primarily due to the increase in blood flow rate Pe_0 rather than metabolic heat γ. For example, at the mid-section $\xi = 0.5$, $\theta(0.5) = 0.688$ for $Pe_0 = 180$ and $\gamma = 0.6$. For zero metabolic heat ($\gamma = 0$), the mid-section temperature drops slightly to 0.64. (iii) Although solution (p) shows that tissue temperature is governed by the parameters Pe_0 and γ, the two are physiologically related. (iv) The increase in metabolic heat production during exercise results in an increase in cutaneous blood flow. Thus neglecting blood perfusion in the cutaneous layer during vigorous exercise is not a reasonable assumption.

10.4. 5 The *s*-Vessel Tissue Cylinder Model [16]

In the Pennes bioheat equation the arterial supply temperature is set equal to the body core temperature and venous return temperature is approximated by the local tissue temperature. Both approximations have been questioned. On the other hand the Chen-Holmes equation and

Weinbaum-Jiji equation are more complex, requiring detailed vascular data and have limited range of applicability. Furthermore, the Weinbaum-Jiji equation is limited to peripheral tissue less than 2 cm thick. These shortcomings motivated further search for a more tractable equation. The *s-vessel tissue cylinder model* addresses some of these issues [16]. An important contribution of this model is the development of a rational theory for the determination of the venous return temperature.

(a) The Basic Vascular Unit. Comprehensive anatomical studies on the vascular geometry of different types of skeletal muscles have identified significant common arrangements [17]. Fig. 10.10 is a schematic representation of the vascular structure in the cat tenuissimus muscle. The sizes of the thermally significant vessels are indicated. The main supply artery and vein *SAV* branch into primary pairs *P*. The *P* vessels branch into secondary pairs *s* which run roughly parallel to the surface. Terminal arterioles and venules *t* branch off the *s* vessels to feed and drain the capillary beds *c* in the tissue. Blood flow in the *SAV*, *P*, and *s* vessels is countercurrent.

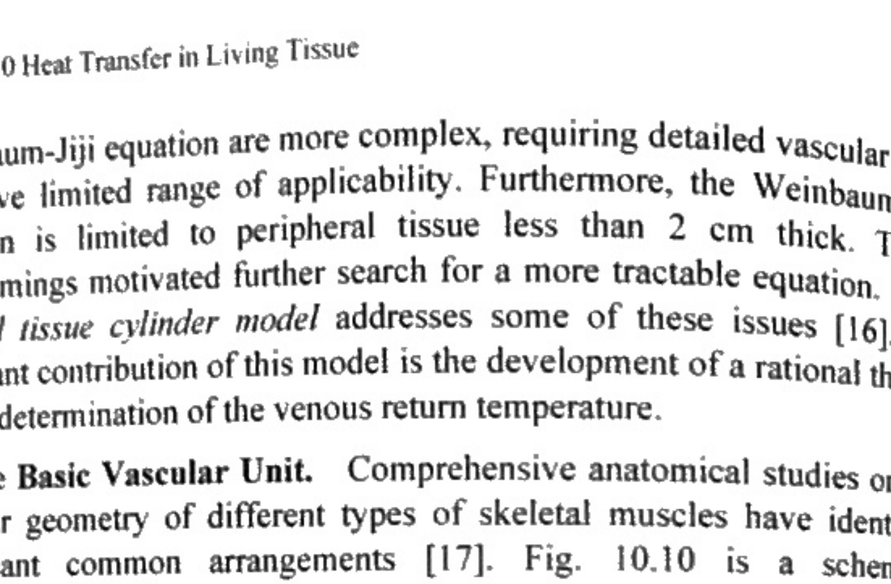

Fig. 10.10 Schematic of a representative vascular arrangement (From [17] with permission.]

The vascular arrangement shown in Fig. 10.10 has an important feature which is central to the formulation of the new model for tissue heat transfer. Each countercurrent *s* pair is surrounded by a cylindrical tissue

which is approximately 1000 μm in diameter. The length of the cylinder depends on the spacing of the *P* vessels along the *SAV* pair, which is typically 10-15 mm. The tissue is a matrix of numerous fibers, arterioles, venules and capillary beds. Attention is focused on this repetitive tissue cylinder as the basic heat exchange unit found in most skeletal muscles. Formulation of a bioheat equation for this basic unit can be viewed as the governing equation for the temperature distribution in the aggregate of all cylinders comprising the muscle.

(b) Assumptions. To formulate a bioheat equation for the tissue cylinder, the following assumptions are made: (1) bleed-off blood flow rate in vessels leaving the artery is equal to that returning to the vein and is uniformly distributed along each pair of *s* vessels, (2) negligible axial conduction through vessels and tissue cylinder, (3) radii of the *s* vessels do not vary along the tissue cylinder, (4) changes in temperature between the inlet to the *P* vessels and the inlet to the tissue cylinder is negligible, (5) the temperature field in the tissue cylinder is based on pure radial conduction with a heat-source pair representing the *s* vessels, and (6) the outer surface of the cylinder is at uniform temperature T_{local}.

(c) Formulation. The capillaries, arterioles and venules (*t* vessels) are essentially in local thermal equilibrium with the surrounding tissue. However, the pair of *s* vessels within the cylinder is thermally significant having blood temperatures that are different from tissue temperature. Three temperature variables are needed to describe the temperature distribution in the tissue cylinder: arterial temperature T_a, venous temperature T_v and tissue temperature T. Fig. 10.11 shows a tissue cylinder and its cross

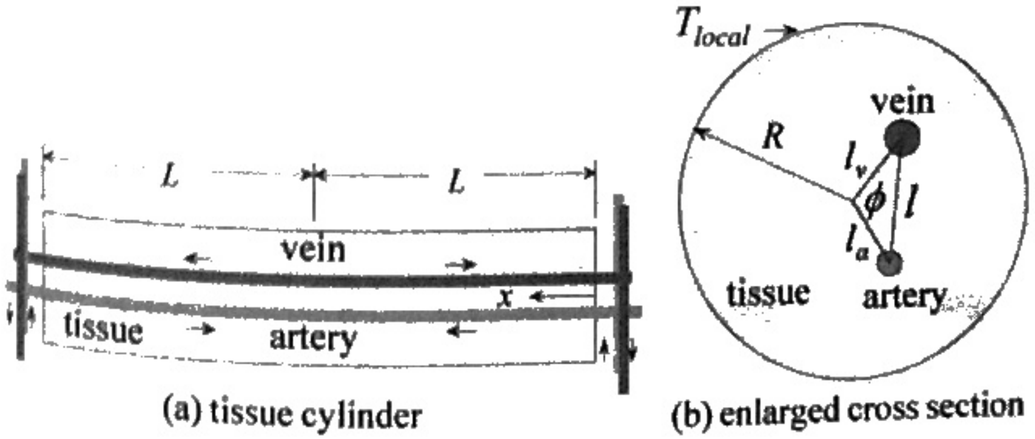

(a) tissue cylinder (b) enlarged cross section

Fig. 10.11

section containing a pair of s vessels. Three governing equations for the temperature field in the s vessels and tissue cylinder were formulated [12]. The two-dimensional velocity field of the axially changing Poiseuille flow in the s vessels was independently determined from the solution to the Navier-Stokes equations. Continuity of temperature and flux at the surfaces of the vessels provides two boundary conditions in the radial direction r. Tissue temperature at the outer radius R of the cylinder is assumed uniform equal to T_{local}. Turning to the boundary conditions in the axial direction x, note that each cylinder extends a distance $x = 2L$ between two neighboring P vessels (see Fig. 10.11). Thus there is symmetry about the mid-plane $x = L$. At the inlet to the cylinder, $x = 0$, the bulk temperature of the artery T_{ab0} is specified. At $x = L$ the flow in the s vessels vanishes and the artery, vein and tissue are in thermal equilibrium at the local tissue temperature T_{local}.

(d) Solution. The three differential equations for the artery, vein and tissue temperature were solved analytically [16]. The most important aspect of the solution is the determination of T_{vb0}, the outlet bulk temperature of the vein at $x = 0$. The importance of this finding will become clear later. For simplicity, we will present only the results for the special case of equal size blood vessels symmetrically positioned relative to the center of the cylinder, i.e., $l_a = l_v$ (see Fig. 10.11). For this case the dimensionless artery-vein temperature difference, ΔT^* at $x = 0$ is given by

$$\Delta T^* = \frac{T_{ab0} - T_{vb0}}{T_{ab0} - T_{local}} = 1 + \frac{A_{11}}{A_{12}} + \sqrt{\frac{A_{11}^2}{A_{12}^2} - 1}, \tag{10.18}$$

where

$$A_{11} = -\frac{1}{4}\left\{\ln\left[R\left(1 - \frac{l_a^2}{R^2}\right)\right] + \frac{11}{24}\right\}, \tag{10.19}$$

$$A_{12} = \frac{1}{4}\ln\left[\frac{R}{l}\sqrt{1 - \frac{2l_a^2\cos\phi}{R^2} + \frac{l_a^4}{R^4}}\right], \tag{10.20}$$

where ϕ, l_a and l (vessel center to center spacing) are defined in Fig. 10.11.

(d) Modification of Pennes Perfusion Term. With the venous return temperature T_{vb0} determined, application of conservation of energy to the blood at $x = 0$ gives the total energy q_b delivered by the blood to the tissue cylinder

$$q_b = \rho_b c_b \pi a_a^2 u_a (T_{ab0} - T_{vb0}), \tag{10.21}$$

where

a_a = artery radius
u_a = average artery blood velocity at $x = 0$

Using eq. (10.18) to express the temperature difference $(T_{ab0} - T_{vb0})$ in terms of ΔT^*, eq. (10.21) becomes

$$q_b = \rho_b c_b \pi a_a^2 u_a \Delta T^* (T_{ab0} - T_{local}).$$

Dividing through by the volume of the cylinder gives

$$\frac{q_b}{\pi R^2 L} = \rho_b c_b \frac{\pi a_a^2 u_a}{\pi R^2 L} \Delta T^* (T_{ab0} - T_{local}). \tag{10.22}$$

Energy generation due to blood flow per unit tissue volume, q_b''', and volumetric blood flow per unit tissue volume $\dot{w}_b$ are

$$q_b''' = \frac{q_b}{\pi R^2 L}, \tag{10.23}$$

and

$$\dot{w}_b = \frac{\pi a_a^2 u_a}{\pi R^2 L}. \tag{10.24}$$

Substituting eq.(10.23) and eq.(10.24) into eq.(10.22) gives

$$q_b''' = \rho_b c_b \dot{w}_b \Delta T^* (T_{ab0} - T_{local}). \tag{10.25}$$

Since $R >> l$, T_{local} is approximately equal to the local average tissue temperature T. Thus, eq. (10.25) becomes

$$q_b''' = \rho_b c_b \dot{w}_b \Delta T^* (T_{ab0} - T). \tag{10.26}$$

This result replaces eq. (10.1) which was introduced in the formulation of the Pennes equation. It differs from eq. (10.1) in two respects: First, the artery supply temperature is not set equal to the body core temperature. Second, it includes the ΔT^* factor. Using eq.(10.26) to replace the blood perfusion term in the Pennes equation (10.3) gives the bioheat equation for the s-vessel tissue cylinder model as

$$\nabla \cdot k\nabla T + \rho_b c_b \dot{w}_b \Delta T^* (T_{ab0} - T) + q_m''' = \rho c \frac{\partial T}{\partial t}. \qquad (10.27)$$

The following observations are made regarding this result:

(1) The dimensionless factor ΔT^* is identified as a *correction coefficient*. Its definition in eq.(10.18) shows that it depends only on the vascular geometry of the tissue cylinder. More importantly, it is independent of blood flow rate. The analysis provides a closed-form solution for the determination of this factor. Its value for most muscle tissues ranges from 0.6 to 0.8. Thus the description of microvascular structure needed to apply this equation is much simpler than that required by Chen-Holmes and Weinbaum-Jiji equations.

(2) The model analytically determines the venous return temperature and accounts for contribution of countercurrent heat exchange in the thermally significant vessels.

(3) The artery temperature T_{ab0} appearing in eq. (10.27) is unknown. It is approximated by the body core temperature in the Pennes bioheat equation. Its determination involves countercurrent heat exchange in *SAV* vessels which have diameters ranging from 300 μm to 1000 μm. The determination of T_{ab0} is presented in Reference [18].

(4) While equations (10.5) and (10.6) apply to the cutaneous layer of peripheral tissue, eq. (10.23) applies to the region below the cutaneous layer.

Example 10.3: Surface Heat Loss from Peripheral Tissue.

Fig. 10.12 is a schematic of a peripheral tissue of thickness L with a cutaneous layer of thickness L_1. Blood at a volumetric rate $\dot{w}_b$ per unit tissue volume and temperature T_{ab0} is supplied to the tissue by the primary arteries. Cutaneous plexus supplies blood to the cutaneous layer at a volumetric rate $\dot{w}_{bc}$ and temperature T_{cb0}. Skin surface is maintained at uniform temperature T_s. Assume that blood perfusion $\dot{w}_{cb}$ is uniformly distributed throughout the cutaneous layer, including the skin. Assume

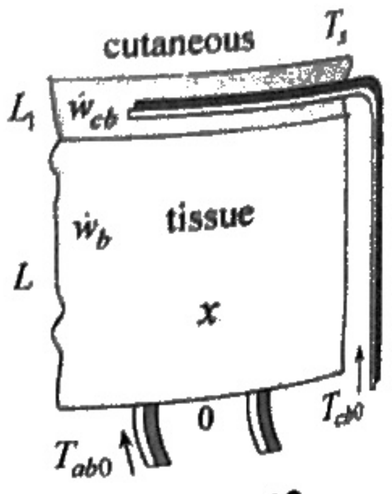

Fig. 10.12

further that metabolic heat production per unit tissue volume is q_m''' and neglect metabolic heat in the cutaneous layer. Using the s-vessel tissue cylinder model, determine surface heat flux for a specified correction coefficient ΔT^*.

(1) Observations. (i) Surface heat flux can be determined once the temperature distribution in the tissue is known. (ii) This is a two layer composite problem: tissue and cutaneous.

(2) Origin and Coordinates. Fig. 10.12 shows the origin and coordinate x.

(3) Formulation

(i) Assumptions. (1) All assumptions leading to bioheat equations (10.5) and (10.27) are applicable, (2) steady state, (3) one-dimensional, (4) constant properties, (5) uniform metabolic heat in the tissue layer, (6) negligible metabolic heat in the cutaneous layer, (7) uniform blood perfusion throughout the cutaneous layer, (8) tissue temperature at the base $x = 0$ is equal to T_{ab0} and (9) specified surface temperature.

(ii) Governing Equations. Application of Fourier's law at the surface gives surface heat flux

$$q_s'' = -k \frac{\partial T_1 (L + L_1)}{\partial x}, \qquad (a)$$

where

k = tissue conductivity
q_s'' = surface heat flux
T_1 = temperature distribution in the cutaneous layer

Two equations are needed to determine the temperature distribution: one for the tissue layer and one for the cutaneous layer. For the tissue layer eq. (10.27) gives

$$\frac{d^2T}{dx^2} + \frac{\rho_b c_b \dot{w}_b \Delta T^*}{k}(T_{ab0} - T) + \frac{q_m'''}{k} = 0, \qquad 0 \le x \le L, \qquad (b)$$

where T is the temperature distribution in the tissue layer. Treating the cutaneous layer as a single region having uniform blood perfusion throughout, equation (10.5) gives

$$\frac{d^2T_1}{dx} + \frac{\rho_b c_b \dot{w}_{cb}}{k}(T_{cb0} - T_1) = 0, \qquad L \le x \le L + L_1. \qquad (c)$$

(iii) Boundary Conditions. Four boundary conditions are required for eqs. (b) and (c)

$$T(0) = T_{ab0}, \tag{d}$$

$$T(L) = T_1 L), \tag{e}$$

$$\frac{dT(L)}{dx} = \frac{dT_1(L)}{dx}, \tag{f}$$

$$T_1(L + L_1) = T_s. \tag{g}$$

(4) Solution. Equations (b) and (c) are rewritten in dimensionless form using the following dimensionless variables

$$\theta = \frac{T - T_{ab0}}{T_s - T_{ab0}}, \quad \phi = \frac{T_1 - T_{ab0}}{T_s - T_{ab0}}, \quad \xi = \frac{x}{L}. \tag{h}$$

Substituting (h) into (b) and (c) gives

$$\frac{d^2\theta}{d\xi^2} - \frac{\rho_b c_b \dot{w}_b L^2}{k} \Delta T^* \theta - \frac{q_b''' L^2}{k(T_{ab0} - T_s)} = 0, \quad 0 \le \xi \le 1, \tag{i}$$

and

$$\frac{d^2\phi}{d\xi^2} - \frac{\rho_b c_b \dot{w}_{cb} L^2}{k}\left[\phi - \frac{T_{ab0} - T_{cb0}}{T_{ab0} - T_s}\right] = 0, \quad 1 \le \xi \le 1 + \xi_0. \tag{j}$$

Introduce the following definitions of the dimensionless parameters in (i) and (j)

$$\beta = \frac{\rho_b c_b \dot{w}_b L^2}{k}, \quad \beta_c = \frac{\rho_b c_b \dot{w}_{cb} L^2}{k},$$
$$\gamma = \frac{q_m''' L^2}{k(T_{ab0} - T_s)}, \quad \lambda = \frac{T_{ab0} - T_{cbo}}{T_{ab0} - T_s}. \tag{k}$$

Substituting (k) into (i) and (j)

$$\frac{d^2\theta}{d\xi^2} - \beta \Delta T^* \theta - \gamma = 0, \quad 0 \le \xi \le 1, \tag{m}$$

$$\frac{d^2\phi}{d\xi^2} - \beta_c \phi + \beta_c \lambda = 0, \quad 1 \le \xi \le 1 + \xi_0, \tag{n}$$

where

$$\xi_0 = \frac{L_1}{L}. \tag{o}$$

Boundary conditions (d)-(g) transform to

$$\theta(0) = 0, \tag{p}$$

$$\theta(1) = \phi(1), \tag{q}$$

$$\frac{d\theta(1)}{dx} = \frac{d\phi(1)}{dx}, \tag{r}$$

$$\phi(1 + \xi_0) = 1. \tag{s}$$

The solutions to (m) and (n) are

$$\theta = A \sinh\sqrt{\beta\Delta T^*}\,\xi + B \cosh\sqrt{\beta\Delta T^*}\,\xi - \frac{\gamma}{\beta\Delta T^*}, \tag{t}$$

$$\phi = C \sinh\sqrt{\beta_c}\,\xi + D \cosh\sqrt{\beta_c}\,\xi + \lambda. \tag{u}$$

where A, B, C and D are constants of integration. Application of boundary conditions (p)-(s) gives the four constants

$$A = \frac{\lambda + \dfrac{(1-\lambda)\cosh\sqrt{\beta_c}}{\cosh\sqrt{\beta_c}(1+\xi_0)} + \dfrac{\lambda\left[1 - \cosh\sqrt{\gamma\Delta T^*}\right]}{\beta\Delta T^*} + C_1 C_2 C_3}{\sinh\sqrt{\beta\Delta T^*} - C_2 C_3 \sqrt{\beta\Delta T^*}\cosh\sqrt{\beta\Delta T^*}}, \tag{v}$$

$$B = \frac{\gamma}{\beta\Delta T^*}, \tag{w}$$

$$C = \left[A\sqrt{\beta\Delta T^*}\cosh\sqrt{\omega\beta\Delta T^*} + C_1\right]C_2, \tag{x}$$

$$D = \frac{1-\gamma}{\cosh\sqrt{\beta_c}(1+\xi_0)} - C_2\left[A\sqrt{\beta\Delta T^*}\cosh\sqrt{\beta\Delta T^*} + C_1\right]\tanh\sqrt{\beta}(1+\xi_0). \tag{y}$$

The constants C_1, C_2 and C_3 are given by

$$C_1 = \frac{\gamma}{\sqrt{\beta \Delta T^*}} \sinh \sqrt{\beta \Delta T^*} - \frac{(1-\lambda)\sqrt{\beta_c} \sinh \sqrt{\beta_c}}{\cosh \sqrt{\beta_c}(1+\xi_0)},$$

$$C_2 = \left\{ \sqrt{\beta_c} \left[\cosh \sqrt{\beta_c} - \sinh \sqrt{\beta_c} \tanh \sqrt{\beta_c}(1+\xi_0) \right] \right\}^{-1},$$

$$C_3 = \sinh \sqrt{\beta_c} - \cosh \sqrt{\beta_c} \tanh \sqrt{\beta_c}(1+\xi_0).$$

Surface heat flux is determined by substituting (u) into (a)

$$\frac{q_s'' L}{k(T_{ab0} - T_s)} = \sqrt{\beta_c} \left[C \cosh \sqrt{\beta_c}(1+\xi_0) + D \sinh \sqrt{\beta_c}(1+\xi_0) \right]. \quad (z)$$

(5) Checking. *Dimensional check*: The parameters $\beta, \beta_c, \gamma, \lambda,$ and ξ_0 and the arguments of the sinh and cosh are dimensionless.

Limiting check: For the special case of $T_s = T_{ab0} = T_{ac0}$ and $q_b''' = 0$, solutions (t), (u) and (z) reduce to the expected results of $T(x) = T_1(x) = T_{ab0}$ and $q_s'' = 0$.

(5) Comments. (i) The solution is characterized by five parameters: $\beta, \beta_c, \gamma, \lambda,$ and ξ_0. (ii) Equation (z) can be used to examine the effect of cutaneous blood perfusion on surface heat flux. Changing blood flow rate through the cutaneous layer is an important mechanism for regulating body temperature. (iii) The solution does not apply to the special case of zero blood perfusion rate since β and β_c appear in the differential equations as coefficients of the variables θ and ϕ, respectively. To obtain the solution to this case, β and β_c must be set equal to zero in equations (m) and (n) prior to solving them.

REFERENCES

[1] Pennes, H.H., "Analysis of Tissue and Arterial Blood Temperatures in the Resting Forearm," *J. Applied Physiology*, vol. 1, pp. 93-122, 1948.

[2] Wulff, W. "The Energy Conservation Equation for Living Tissues," *IEEE Transactions of Biomedical Engineering*, BME-21, pp. 494-495, 1974.

[3] Weinbaum, S., and Jiji, L.M., "A Two Phase Theory for the Influence of Circulation on the Heat Transfer in Surface Tissue," *In, 1979 Advances in Bioengineering* (M.K. Wells, ed.), pp. 179-182, ASME, New York, 1979.

[4] Klinger, H.G., "Heat Transfer in Perfused Biological Tissue-1: General Theory," *Bulletin of Mathematical Biology*, vol. 36, pp. 403-415, 1980.

[5] Chen, M.M., and Holmes, K.R., "Microvascular Contributions in Tissue Heat Transfer," *Annals of the New York Academy of Sciences*, vol., 335, pp. 137-150, 1980.

[6] Charny, C.K., Weinbaum, S., and Levin, R.L., "An Evaluation of the Weinbaum-Jiji Bioheat Equation for Normal and Hyperthermic Conditions," *ASME J. of Biomechanical Engineering*, vol. 112, pp. 80-87, 1990.

[7] Jiji, L.M., Weinbaum, S., and Lemons, D.E., "Theory and Experiment for the Effect of Vascular Microstructure on Surface tissue Heat Transfer-Part II: Model Formulation and Solution," *ASME J. of Biomechanical Engineering*, vol., 106, pp. 331-341, 1984.

[8] Weinbaum, S., and Jiji, L.M., "A New Simplified Bioheat Equation for the Effect of Blood Flow on Local Average Tissue Temperature," *ASME J. of Biomechanical Engineering*, vol. 107, pp. 131-139, 1985.

[9] Weinbaum, S., Jiji, L.M., and Lemons, D.E., "Theory and Experiment for the Effect of Vascular Microstructure on Surface Tissue Heat Transfer-Part I: Anatomical Foundation and Model Conceptualization," *ASME J. of Biomechanical Engineering*, vol., 106, pp. 321-330, 1984.

[10] Weinbaum, S., and Lemons, D.E., "Heat Transfer in Living Tissue: The Search for a Blood-Tissue Energy Equation and the Local Thermal Microvascular Control Mechanism," *BMES Bulletin*, vol. 16, no. 3, pp. 38-43, 1992

[11] Arkin, H., Xu, L.X., and Holmes, K.R., "Recent Development in Modeling Heat Transfer in Blood Perfused Tissue," *IEEE Transactions on Biomedical Engineering*, vol. 41, no. 2, pp.97-107, 1994.

[12] Dagan, Z., Weinbaum, S., and Jiji, L.M., "Parametric Studies on the Three-Layer Microcirculatory Model for Surface Tissue Energy

Exchange," *ASME J. Biomechanical Engineering*, vol. 108, pp. 89-96, 1986.

[13] Chato, J.C. "Heat Transfer to Blood Vessels," *ASME J. Biomechanical Engineering*, vol. 102, pp. 110-118, 1980.

[14] Song, J., Xu, L.X., Lemons, D.E., and Weinbaum, S., "Enhancement in the Effective Thermal Conductivity in Rat Spinotrapezius Due to Vasoregulation," *ASME J. of Biomechanical Engineering*, vol. 119, pp. 461-468, 1997.

[15] Song, W.J., Weinbaum, S., and Jiji, L.M., "A Theoretical Model for Peripheral Tissue Heat Transfer Using the Bioheat Equation of Weinbaum and Jiji," *ASME J. of Biomechanical Engineering*, vol. 109, pp. 72-78, 1987.

[16] Weinbaum, S., Xu, L.X., Zhu, L., and Ekpene, A., " A New Fundamental Bioheat Equation for Muscle Tissue: Part I: Blood Perfusion Term," *ASME J. Biomechanical Engineering*, vol. 119, pp.278-288, 1997.

[17] Myrhage, R., and Eriksson, E., "Arrangement of the Vascular Bed in Different Types of Skeletal Muscles, " *Progress in Applied Microcirculation*, vol. 5, pp.1-14, 1984.

[18] Zhu, L., Xu, L.X., He, Q., and Weinbaum, S., "A New Fundamental Bioheat Equation for Muscle Tissue: Part II: Temperature of SAV Vessels," *ASME J. Biomechanical Engineering*, vol. 124, pp.121-132, 2002.

[19] Farlow, J.O., Thompson, C.V., and Rosner, D.E., "Plates of the Dinosaur Stegosaurus: Forced Convection Heat Loss Fins?", Science, vol. 192, pp.1123-1125, 1976.

PROBLEMS

10.1 Pennes[1] obtained experimental data on temperature distribution in the forearm of several subjects. The average center and skin surface temperatures were found to be $36.1\,^{\circ}\mathrm{C}$ and $33.6\,^{\circ}\mathrm{C}$, respectively. Use the Pennes model to predict these two temperatures based on the following data:

c_b = specific heat of blood = 3.8 J/g–°C
h = heat transfer coefficient = $4.18\,\mathrm{W/m^2}$–°C
k_b = thermal conductivity of blood = 0.5 W/m–°C
k = thermal conductivity of muscle = 0.5 W/m–°C
q_m''' = metabolic heat production = $0.000418\,\mathrm{W/cm^3}$
R = average forearm radius = 4 cm
$T_{a0} = 36.3\,^{\circ}\mathrm{C}$
$T_\infty = 26.6\,^{\circ}\mathrm{C}$
$\dot{w}_b$ = volumetric blood perfusion rate per unit tissue volume
$= 0.0003\,\mathrm{cm^3/s/cm^3}$
ρ_b = blood density = $1050\,\mathrm{kg/m^3}$

10.2 Blood perfusion rate plays an important role in regulating body temperature and skin heat flux. Use Pennes's data on the forearm of Problem 10.1 to construct a plot of skin surface temperature and heat flux for blood perfusion rates ranging from $\dot{w}_b = 0$ to $w_b = 0.0006\ (\mathrm{cm^3/s})/\mathrm{cm^3}$.

10.3 Certain clinical procedures involve cooling of human legs prior to surgery. Cooling is accomplished by maintaining surface temperature below body temperature. Model the leg as a cylinder of radius R with volumetric blood perfusion rate per unit tissue volume $\dot{w}_b$ and metabolic heat production rate q_m'''. Assume uniform skin surface temperature T_s. Use the Pennes bioheat equation to determine the steady state one-dimensional temperature distribution in the leg.

10.4 A manufacturer of suits for divers is interested in evaluating the effect of thermal conductivity of suit material on skin temperature. Use Pennes model for the forearm to predict skin surface temperature of a diver wearing a tight suit of thickness δ and thermal conductivity k_o. The volumetric blood perfusion rate per unit tissue volume is $\dot{w}_b$ and metabolic heat production rate is q_m'''. The ambient temperature is T_∞ and the heat transfer coefficient is h. Neglect curvature of the suit layer.

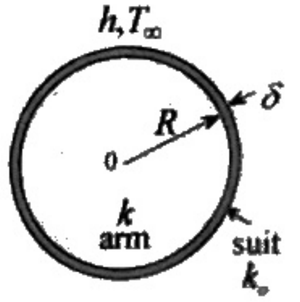

10.5 Consider the single layer model of the peripheral tissue of Example 10.2. Tissue thickness is L and blood supply temperature to the deep layer at $x = 0$ is T_{a0}. The skin surface exchanges heat by convection. The ambient temperature is T_∞ and the heat transfer coefficient is h. Assume that the vascular geometry function $V(\xi)$ can be approximated by

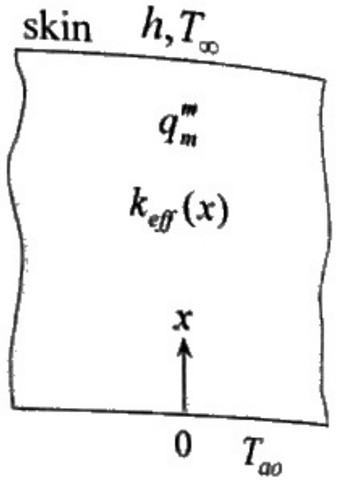

$$V(\xi) = A + B\xi + C\xi^2,$$

where

$$A = 6.32\times10^{-5},\ B = -15.9\times10^{-5},\ \text{and}\ C = 10\times10^{-5}.$$

Use the Weinbaum-Jiji simplified bioheat equation to obtain a solution to the temperature distribution in the tissue. Express the result in non-dimensional form using the following dimensionless quantities:

$$\theta = \frac{T - T_\infty}{T_{a0} - T_\infty},\quad \xi = \frac{x}{L},\quad \gamma = \frac{q'''_m L^2}{k(T_{a0} - T_\infty)},\quad Bi = \frac{hL}{k},$$

$$Pe_0 = \frac{2\rho_b c_b a_0 u_0}{k_b}.$$

Construct a plot showing the effect of Biot number (surface convection) on tissue temperature distribution $\theta(\xi)$ for $Pe_0 = 180$, $\gamma = 0.6$ and $Bi = 0.1$ and 1.0.

10.6 In Example 10.3 skin surface is maintained at specified temperature. To examine the effect of surface convection on skin surface heat flux, repeat Example 10.3 assuming that the skin exchanges heat with the surroundings by convection. The ambient temperature is T_∞ and the heat transfer coefficient is h.

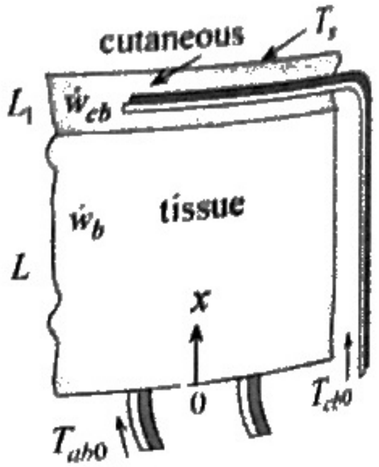

10.7 The vascular geometry of the peripheral tissue of Example 10.2 is approximated by a polynomial function. To evaluate the sensitivity of temperature distribution to the assumed vascular geometry function, consider a linear representation of the form

$$V(\xi) = A + B\xi,$$

where $A = 6.32\times10^{-5}$ and $B = -6.32\times10^{-5}$. Determine k_{eff}/k and $\theta(\xi)$ for $\gamma = 0.6$ and $Pe_0 = 180$. Compare your result with Example 10.2.

10.8 A digit consists mostly of bone surrounded by a thin cutaneous layer. A simplified model for analyzing the temperature distribution and heat transfer in digits is a cylindrical bone covered by a uniform cutaneous layer. Neglecting axial and angular variations, the problem reduces to one-dimensional temperature distribution. Consider the case of a digit with negligible metabolic heat production. The skin surface exchanges heat with the ambient by convection. The heat transfer coefficient is h and the ambient temperature is T_∞. Using the Pennes equation determine the steady state temperature distribution and heat transfer rate. Note that in the absence of metabolic heat production the bone in this model is at uniform temperature.

10.9 Fin approximation can be applied in modeling organs such as the elephant ear, rat tail, chicken legs, duck beak and human digits. Temperature distribution in these organs is three-dimensional. However, the problem can be significantly simplified using fin approximation. As an example, consider the rat tail. Anatomical studies have shown that it consists of three layers: bone, tendon and cutaneous layer. There are three major axial artery-vein pairs: one ventral and two lateral. These pairs are located in the tendon near the cutaneous layer as shown. The ventral vein is small compared to the lateral veins, and the lateral arteries are small compared to the ventral artery. Blood perfusion from the arteries to the veins takes place mostly in the cutaneous layer through a network of small vessels. Assume that blood is supplied to the cutaneous layer at

uniform temperature T_{a0} all along the tail. Blood equilibrates at the local cutaneous temperature T before returning to the veins. Assume further that (1) cutaneous layer, tendon and bone have the same conductivity, (2) negligible angular variation, (3) uniform blood perfusion along the tail, (4) negligible metabolic heat, (5) steady state, (6) uniform outer radius and (7) negligible temperature variation in the radial direction (fin approximation is valid, $Bi << 1$). Surface heat exchange is by convection. The heat transfer coefficient is h and the ambient temperature is T_∞. Using Pennes model for the cutaneous layer, show that the heat equation for the rat tail is given by

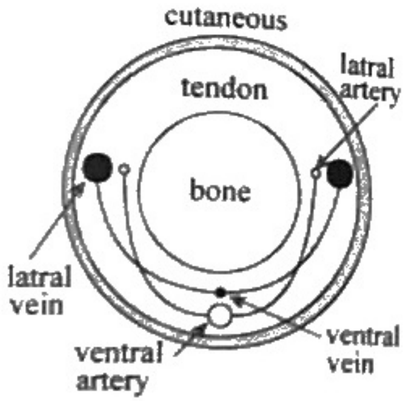

$$\frac{d^2\theta}{d\xi^2} - (m+\beta)\theta + m = 0,$$

where

$$\theta = \frac{T - T_{a0}}{T_\infty - T_{a0}}, \quad \xi = \frac{x}{L},$$

$$m = \frac{2hL^2}{kR}, \quad \beta = \frac{\dot{w}_b \rho_b c_b L^2}{k}.$$

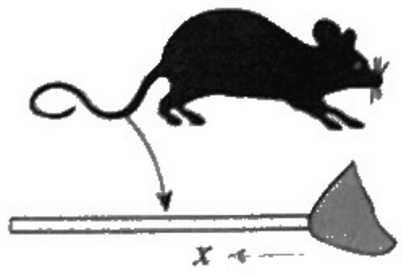

Here L is tail length, R tail radius and x is axial distance along the tail.

10.10 Consider the rat tail model described in Problem 10.9. Assume that the base of the tail is at the artery supply temperature T_{a0} and that the tip is insulated. Show that the axial temperature distribution and total heat transfer rate from the tail are given by

$$\theta(\xi) = \frac{m}{\beta + m}\left[(\tanh\sqrt{\beta+m})\sinh\sqrt{\beta+m}\,\xi - \cosh\sqrt{\beta+m}\,\xi + 1\right],$$

and

$$q = 2\pi hRL(T_{a0} - T_\infty)\left[1 - \frac{m}{\beta+m} + \frac{m\tanh\sqrt{\beta+m}}{(\beta+m)\sqrt{\beta+m}}\right],$$

Construct a plot of the axial temperature distribution and calculate the heat transfer rate for the following data:

$$c_b = 3.8\frac{\text{J}}{\text{g}-^\circ\text{C}}, \quad h = 15.9\frac{\text{W-m}^2}{^\circ\text{C}}, \quad k = 0.5\frac{\text{W-m}}{^\circ\text{C}},$$

$$L = 22.5\,\text{cm}, \quad R = 0.365\,\text{cm}, \quad T_{a0} = 36\,^\circ\text{C}, \quad T_\infty = 22.5\,^\circ\text{C},$$

$$\dot{w}_b = 0.01947\frac{\text{cm}^3/\text{s}}{\text{cm}^3}, \quad \rho = 1.05\frac{\text{g}}{\text{cm}^3}.$$

10.11 Studies have shown that blood perfusion along the rat tail is non-uniform. This case can be analyzed by dividing the tail into sections and assigning different blood perfusion rate to each section. Consider the rat tail described in Problem 10.9. Model the tail as having two sections. The first section extends a length L_1 from the base and the second has a length of $(L - L_1)$. Blood perfusion rate in the first section is $\dot{w}_{b1}$ and in the second section $\dot{w}_{b2}$. Determine the axial temperature distribution in the tail in terms of the following dimensionless quantities

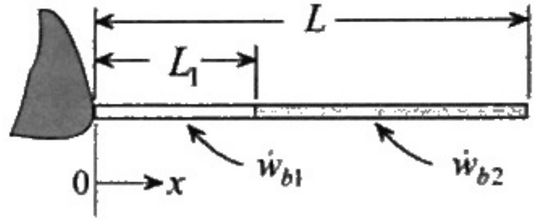

$$\theta = \frac{T - T_{a0}}{T_\infty - T_{a0}}, \quad \xi = \frac{x}{L}, \quad \xi_1 = \frac{L_1}{L}, \quad m = \frac{2hL^2}{kR},$$

$$\beta_1 = \frac{\dot{w}_{b1}\rho_b c_b L^2}{k}, \quad \beta_2 = \frac{\dot{w}_{b2}\rho_b c_b L^2}{k}.$$

10.12 The cutaneous layer of a peripheral tissue is supplied by blood at temperature T_{c0} and a *total* flow rate $\dot{W}_{cb}$. The tissue is supplied by blood at temperature T_{a0} and *total* flow rate $\dot{W}_b$. Tissue thickness is L and cutaneous layer thickness is L_1. One mechanism for regulating surface heat loss is by controlling blood flow through the cutaneous layer. Use the Weinbaum-Jiji simplified bioheat equation

to examine the effect of blood flow ratio, $R = \dfrac{\dot{W}_{cb}}{W_b} = \dfrac{L_1 \dot{w}_{cb}}{L \dot{w}_b}$, on surface heat flux. The skin is maintained at uniform temperature T_s. Assume a linear tissue vascular geometry function of the form

$$V(\xi) = A + B\xi .$$

10.13 Studies have concluded that the plates on the back of the dinosaur Stegosaurus served a thermoregulatory function as heat dissipating fins [19]. There are indications that the network of channels within the plates may be blood vessels. Model the plate as a rectangular fin of width W, length L and thickness t. Use the Pennes model to formulate the heat equation for this blood perfused plate. The plate exchanges heat with the ambient air by convection. The heat transfer coefficient is h and the ambient temperature is T_∞. Assume that blood reaches each part of the plate at temperature T_{a0} and that it equilibrates at the local temperature T. Assume further that (1) blood perfusion is uniform, (2) negligible metabolic heat production, (3) negligible temperature variation along plate thickness t (fin approximation is valid, $Bi << 1$), (4) steady state and (5) constant properties. Show that the heat equation for this model is given by

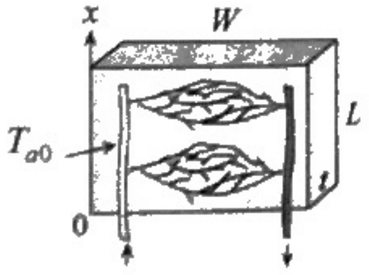

$$\frac{d^2\theta}{d\xi^2} - (m+\beta)\theta + m = 0,$$

where

$$\theta = \frac{T - T_{a0}}{T_\infty - T_{a0}}, \quad \xi = \frac{x}{L}, \quad m = \frac{2h(W+t)L^2}{kWt}, \quad \beta = \frac{\dot{w}_b \rho_b c_b L^2}{k}.$$

10.14 Modeling the plates on the back of the dinosaur Stegosaurus as rectangular fins, use the bioheat fin equation formulated in Problem 10.13 to show that the enhancement in heat transfer, η, due to blood flow is given by

$$\eta = \frac{q}{q_o} = \frac{\sqrt{m}}{\beta + m} \frac{\beta + \dfrac{m}{\sqrt{\beta + m}} \tanh\sqrt{\beta + m}}{\tanh\sqrt{m}},$$

where

$$m = \frac{2h(W+t)L^2}{kWt}, \quad \beta = \frac{\dot{w}_b \rho_b c_b L^2}{k}.$$

q = heat transfer rate from plate with blood perfusion
q_o = heat transfer rate from plate with no blood perfusion

Compute the enhancement η and total heat loss from 10 plates for the following data:

c_b = specific heat of blood = 3800 J/kg–°C
h = heat transfer coefficient = 14.9 W/m^2–°C
k = thermal conductivity = 0.6 W/m–°C
L = plate length = 0.45 m
t = plate thickness = 0.2 m
T_{a0} = blood supply temperature = 37 °C
T_∞ = ambient temperature = 27 °C
$\dot{w}_b$ = blood perfusion rate per unit tissue volume
= 0.00045 (cm^3/s)/cm^3
W = plate width = 0.7 m
ρ_b = blood density = 1050 kg/m^3

10.15 Elephant ears serve as a thermoregulatory device by controlling blood supply rate to the ears and by flapping them. Increasing blood perfusion increases heat loss due to an increase in surface temperature. Flapping results in an increase in the heat transfer coefficient as air flow over the ears changes from natural to forced convection. Consider the following data on a 2000 kg elephant which generates 1640 W:

c_b = specific heat of blood = 3800 J/kg–°C

h_n = natural convection heat transfer coefficient = 2 W/m^2–°C
h_f = forced convection heat transfer coefficient (flapping)
= 17.6 W/m^2–°C
k = thermal conductivity = 0.6 W/m–°C
L = equivalent length of square ear = 0.93 m
t = average ear thickness = 0.6 cm
T_{a0} = blood supply temperature = 36 °C
T_∞ = ambient temperature = 24 °C
$\dot{w}_b$ = blood perfusion rate per unit tissue volume
= 0.0015 (cm^3/s)/cm^3
ρ_b = blood density = 1050 kg/m^3

Neglecting metabolic heat production in the ear, model the ear as a square fin using the bioheat equation formulated in Problem 10.13 to determine the total heat transfer rate from two sides of two ears with and without flapping. In addition compute the enhancement in heat transfer for the two cases. Define enhancement η as

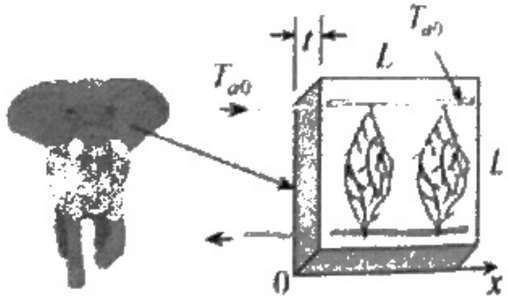

$$\eta = \frac{q}{q_o},$$

where

q = heat transfer rate from ear
q_o = heat transfer rate from ear with no blood perfusion and no flapping

10.16 Cryosurgical probes are used in medical procedures to selectively freeze and destroy diseased tissue. The cryoprobe surface is maintained at a temperature below tissue freezing temperature causing a frozen front to form at the surface and propagate outward. Knowledge of the maximum frozen layer or lesion size is helpful to the surgeon in selecting the proper settings for the cryoproble. Maximum lesion size corresponds to the steady state temperature

distribution. Consider a planar probe which is inserted in a large region of tissue. Probe thickness is L and its surface temperature is T_o. Using the s-vessel tissue cylinder model, determine the maximum lesion size for the following data:

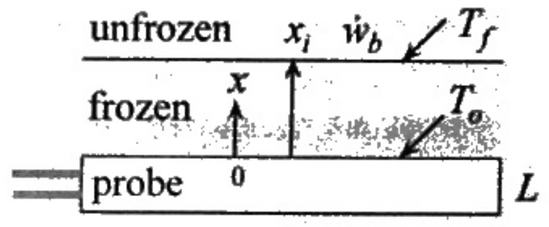

c_b = specific heat of blood = 3800 J/kg–°C
L = probe thickness = 4 mm
k = thermal conductivity of unfrozen tissue = 0.6 W/m–°C
k_s = thermal conductivity of frozen tissue = 1.8 W/m–°C
q_m''' = metabolic heat production = 0.021 W/cm^3
T_{ab0} = artery blood temperature = 36.5 °C
T_f = tissue freezing temperature = 0 °C
T_o = probe surface temperature = –42 °C
$\dot{w}_b$ = blood perfusion rate per unit tissue volume
= 0.0032 (cm^3/s)/cm^3
ρ_b = blood density = 1050 kg/m^3
$\Delta T^* = 0.75$

10.17 A cylindrical cryosurgical probe consists of a tube whose surface temperature is maintained below tissue freezing temperature T_f. The frozen region or lesion around the cryoprobe reaches its maximum size at steady state. Predicting the maximum lesion size is important in avoiding damaging healthy tissue and in targeting diseased areas. Consider a cylindrical probe which is inserted in a large tissue region. Probe radius is r_o and its surface temperature is T_o. Metabolic heat production is q_m''' and blood perfusion rate is $\dot{w}_b$. Let T be the temperature distribution in the unfrozen tissue and T_s the

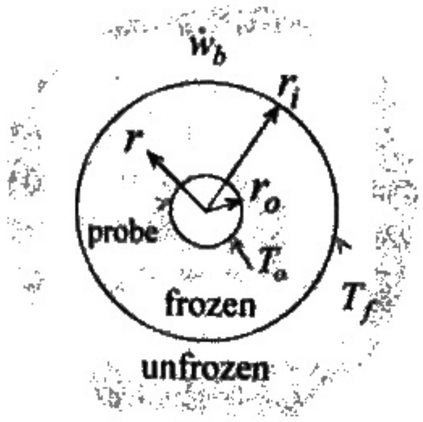

temperature distribution in the frozen tissue. Using the s-vessel tissue cylinder model, determine the steady state temperature distribution in the two regions and the maximum lesion size. Note that the conductivity of frozen tissue k_s is significantly different from the conductivity k of unfrozen tissue. Express the result in dimensionless form using the following dimensionless quantities:

$$\theta = \frac{T - T_{ab0}}{T_f - T_{ab0}}, \quad \theta_s = \frac{T_s - T_o}{T_f - T_o}, \quad \xi = \frac{r}{r_o}, \quad \xi_i = \frac{r_i}{r_o},$$

$$\beta = \frac{\dot{w}_b \rho_b c_b \Delta T^* r_o^{\,2}}{k}, \quad \gamma = \frac{q_m''' r_o^2}{k(T_{ab0} - T_f)}.$$

10.18 A brain surgical procedure requires the use of a spherical cryosurgical probe to create a frozen region (lesion) 6 mm in radius. A 3 mm radius spherical cryoprobe is selected for insertion into the diseased area. Using the Pennes model, determine the required probe surface temperature such that the maximum lesion size does not exceed 6 mm. Note that maximum size corresponds to the steady state temperature distribution in the frozen and unfrozen regions around the probe. The following data is given

c_b = specific heat of blood = 3800 J/kg–°C
k = thermal conductivity of unfrozen tissue = 0.6 W/m–°C
k_s = thermal conductivity of frozen tissue = 1.8 W/m–°C
q_m''' = metabolic heat production = 0.011 W/cm^3
T_{a0} = artery blood temperature = 36.5 °C
T_f = tissue freezing temperature = 0 °C
$\dot{w}_b$ = blood perfusion rate per unit tissue volume
= 0.0083 (cm^3/s)/cm^3
ρ_b = blood density = 1050 kg/m^3

10.19 Analytical prediction of the growth of the frozen region around cryosurgical probes provides important guidelines for establishing probe application time. Consider the planar probe described in Problem 10.16. Use the s-vessel tissue cylinder model and assume a quasi-steady approximation to show that the dimensionless interface location ξ_i is given by:

$$\tau = \frac{1}{\lambda^2}\left[\lambda\xi_i - \ln(1 + \lambda\xi_i)\right],$$

where

$$\tau = \frac{k_s(T_f - T_o)}{\rho L^2 \mathcal{L}} t, \quad \lambda = \sqrt{\beta}\,\frac{k(T_f - T_{ab0})}{k_s(T_f - T_o)}\left[1 + \frac{\gamma}{\beta}\right], \quad \xi_i = \frac{x_i}{L},$$

$$\beta = \frac{\dot{w}_b \rho_b c_b \Delta T^* L^2}{k}, \quad \gamma = \frac{q_m''' L_o^2}{k(T_{ab0} - T_f)}.$$

where $\mathcal{L} = 333{,}690$ J/kg is the latent heat of fusion and $\rho_s = 1040\,\text{kg/m}^3$ is the density of frozen tissue. How long should the probe of Problem 10.16 be applied so that the frozen layer is 3.5 mm thick?

10.20 Consider the cylindrical cryosurgical described in Problem 10.17. Using the s-vessel tissue cylinder model and assuming quasi-steady interface motion, determine lesion size as a function of time.

10.21 The spherical cryosurgical probe of Problem 10.18 is used to create a lesion corresponding to 95% of its maximum size. Using the Pennes model and assuming quasi-steady interface motion, determine the probe application time. Probe temperature is $T_o = -29.6$°C, latent heat of fusion is $\mathcal{L} = 333{,}690$ J/kg and the density of frozen tissue is $\rho_s = 1040\,\text{kg/m}^3$.

10.22 Prolonged exposure to cold environment of elephants can result in frost bite on their ears. Model the elephant ear as a sheet of total surface area (two sides) A and uniform thickness δ. Assume uniform blood perfusion $\dot{w}_b$ and uniform metabolic heat q_m'''. The ear loses heat by convection. The ambient temperature is T_∞ and the heat transfer coefficient is h. Using lumped capacity approximation and the Pennes model, show that the dimensionless transient heat equation is given by

$$\frac{d\theta}{d\tau} = (1+\gamma) - (1+\beta)\theta\,,$$

where

$$\theta = \frac{T - T_{a0}}{T_\infty - T_{a0}},\quad \tau = \frac{2h}{\delta\rho c}t,\quad \beta = \frac{\dot{w}_b \rho_b c_b \delta}{2h},\quad \gamma = \frac{q'''_m \delta}{2h(T_\infty - T_{a0})}.$$

Here ρ is tissue density and c tissue specific heat. The subscript b refers to blood. Determine the maximum time a zoo elephant can remain outdoors on a cold winter day without resulting in frost bite when the ambient temperature is lower than freezing temperature T_f. Assume that initially the ears are at uniform temperature T_i.

11

MICROSCALE CONDUCTION

Chris Dames
Department of Mechanical Engineering
University of California, Riverside

11.1 Introduction

Heat conduction at the microscale can be dramatically different than at the macroscale. The differences become clear by comparing the thermal conductivity of a "bulk" material (that is, a large sample that is by definition free of microscale effects) to the effective thermal conductivity of a microscopic sample of the same material. The values of thermal conductivity that are readily available in textbooks and standard reference books (so-called "handbook values") apply to bulk samples, but must be used with great caution for microscale samples. As one example, according to a standard reference [1], the thermal conductivity k of pure silicon at room temperature is 148 W/m-°C. This value is appropriate for silicon samples with characteristic lengths ranging from meters to millimeters to microns. However, a silicon nanowire of diameter 56 nm ($1\,\text{nm} = 10^{-9}$ m) has thermal conductivity of only 26 W/m-°C [2], a reduction by more than a factor of five compared to the bulk value. The reductions are even more dramatic at low temperature: at 20 K the values are 4940 W/m-°C for bulk Si [1], and 0.72 W/m-°C for the Si nanowire [2], a difference of more than a factor of 6000! By the end of this chapter, readers should understand the physical reasons for this tremendous reduction, and be able to evaluate it numerically with approximate calculations.

Although the great majority of microsystems follow this same pattern of having thermal conductivity less than their bulk counterparts, there are also certain materials that exhibit nanoscale thermal conductivity greater than